ISSN 0015-4628, Fluid Dynamics, 2023, Vol. 58, No. 6, pp. 1033–1041. © The Author(s), 2023. This article is an open access publication.
Russian Text © The Author(s), 2023, published in Izvestiya RAN. Mekhanika Zhidkosti i Gaza, 2023, No. 6, pp. 67–74.

Laminar Swirling Wall Jets

A. M. Gaifullin[a],* and A. S. Shcheglov[a],**

[a]*Central Aerohydrodynamic Institute (TsAGI), Zhukovskii, Moscow oblast, Russia*

**e-mail: gaifullin@tsagi.ru*

***e-mail: shcheglov@phystech.edu*

Received June 5, 2023; revised June 20, 2023; accepted June 25, 2023

Abstract—The problem of determining the characteristics of a laminar swirling wall jet of an incompressible fluid is considered. Numerical solutions of the Navier–Stokes equations are obtained in the stationary and non-statitonary formulations. It is shown that the jet characteristics obey a self-similar law at large distances from the jet source, as in the case of a three-dimensional laminar non-swirling jet, but in our case the jet propagates at a certain angle to the initial direction of jet blowing. With a large swirling of flow in the jet, regions of recirculation flow appear and the jet flow becomes unsteady.

Keywords: wall jet, submerged jet, swirling jet, self-similar solution, recirculation flow, Navier–Stokes equations

DOI: 10.1134/S0015462823602267

Wall jets are the jets propagating along a rigid surface. Despite the practical importance of studying wall jets, a small number of publications are devoted to the study of flow in them. Mainly, these are experimental studies of turbulent wall jets, which can be conventionally divided into plane jets [1–4], three-dimensional non-swirling jets [5–12], and three-dimensional swirling jets [13]. Numerical studies of plane wall jets were carried out in [14, 15] and three-dimensional non-swirling wall jets were numerically studied in [16–19]; the authors are not aware of works on the numerical study of three-dimensional swirling wall jets.

For laminar wall jets, theoretical and numerical studies were carried out only for plane and three-dimensional non-swirling jets. The problem of a non-swirling laminar jet flowing out of a thin slot parallel to the solid surface was first solved in terms of the boundary layer equations [20] and repeated in [21] three years later. The success in solving the problem was facilitated by the fact that in the plane case it was possible to find an invariant that retains its value in any jet cross-section. The presence of the invariant made it possible to theoretically determine the self-similarity parameter responsible for change in the characteristics of the jet along the longitudinal coordinate x, the jet thickness grows proportionally to $x^{3/4}$, while the longitudinal velocity component decays as $x^{-1/2}$.

In the case of the three-dimensional wall jet that flows out from a small source parallel to the solid surface, flow can be described using the parabolic Navier–Stokes equations, in which the non-order terms, namely, the longitudinal pressure gradient and the second derivatives along the longitudinal coordinate in the viscous terms of the equations, are neglected. In [22] an assumption was made that the solution should reach a self-similar regime at large distances from the jet source. But in [22], the law of conservation of the angular momentum of flow was used to determine the self-similarity parameter; actually, this momentum is not conserved. In [23], the value of the self-similarity parameter and various jet characteristics associated with it were obtained. Since for the three-dimensional wall jet no invariant solution has been constructed to date, the self-similarity parameter can be determined only by numerically solving the problem [24]; this was made in [23]. As a rule, in the absence of the invariant, it is impossible to obtain universal characteristics. For example, in the case of the three-dimensional wall jet, the profiles of velocity components and pressure will vary as functions of the shape of the outlet cross-section and its height above the jet outlet plane depending on the velocity profile and the Reynolds number. However, as shown in [23], the universal profiles can still be constructed if one assumes that the invariant, although not found, exists and if there exists an asymptotic solution of the problem in some domains.

In the present paper we will consider three-dimensional swirling laminar wall jets. As a result of the studies, the authors tried to answer the following questions. Do the characteristics in the far field of the jet obey self-similarity laws, and if so, does the self-similarity parameter depend on the swirl of the jet? The line along which the jet propagates in the presence of swirl will no longer be straight line. Is this line in the far field parallel to the x axis along which the jet is blown out, or is it inclined to it at some angle? This article is devoted to the solution of these and some other questions.

1. FORMULATION OF THE PROBLEM.

We will consider steady-state incompressible fluid flow. We will introduce a Cartesian coordinate system x_1, y_1, z_1. In this coordinate system the velocity components will be denoted by u_1, v_1, w_1. We will denote the fluid density by ρ, the pressure p_1, and the kinematic viscosity coefficient by ν. The infinite rigid plane is given by the equation $y_1 = 0$. The jet is blown out of a round cylindrical pipe of radius a in parallel to the rigid plane in the direction of the x_1 axis into submerged space. The center of the inlet pipe cross- section has the coordinates $x_1 = 0$, $y_1 = h_1$, $z_1 = 0$. Similarly to [25], the jet is swirled by rotating the inner surface of the pipe. The outer surface of the pipe does not rotate. At the outlet pipe cross-section, the jet is swirled clockwise from the flow side.

We will define the dimensionless coordinates and variables

$$x = \frac{x_1}{a}, \quad y = \frac{y_1}{a}, \quad z = \frac{z_1}{a}, \quad \mathbf{V} = \frac{\mathbf{V}_1}{u_{1*}}, \quad p = \frac{p_1 - p_{1\infty}}{\rho u_{1*}^2}, \quad \mathrm{Re} = \frac{u_{1*}a}{\nu},$$

where u_{1*} is the average-flow-rate velocity of fluid in the pipe.

The fluid flow will be considered to be laminar, its characteristics must satisfy the Navier–Stokes equations

$$\mathrm{div}\mathbf{V} = 0, \quad (\mathbf{V}\nabla)\mathbf{V} = -\mathrm{grad}p + \mathrm{Re}^{-1}\Delta\mathbf{V}. \tag{1.1}$$

In [23] it was also shown that the characteristics of the three-dimensional wall jet at high Reynolds numbers can be determined in the approximation of parabolic equations

$$\frac{\partial u}{\partial x} + \frac{\partial v}{\partial y} + \frac{\partial w}{\partial z} = 0, \tag{1.2}$$

$$u\frac{\partial u}{\partial x} + v\frac{\partial u}{\partial y} + w\frac{\partial u}{\partial z} = \frac{1}{\mathrm{Re}}\left(\frac{\partial^2 u}{\partial y^2} + \frac{\partial^2 u}{\partial z^2}\right), \tag{1.3}$$

$$u\frac{\partial v}{\partial x} + v\frac{\partial v}{\partial y} + w\frac{\partial v}{\partial z} = -\frac{\partial p}{\partial y} + \frac{1}{\mathrm{Re}}\left(\frac{\partial^2 v}{\partial y^2} + \frac{\partial^2 v}{\partial z^2}\right), \tag{1.4}$$

$$u\frac{\partial w}{\partial x} + v\frac{\partial w}{\partial y} + w\frac{\partial w}{\partial z} = -\frac{\partial p}{\partial z} + \frac{1}{\mathrm{Re}}\left(\frac{\partial^2 w}{\partial y^2} + \frac{\partial^2 w}{\partial z^2}\right). \tag{1.5}$$

In the case of the non-swirling three-dimensional wall jet, at large x the solution of Eqs. (1.2)–(1.5) tends to the following self-similar solution with the self-similarity parameter equal to 4/3:

$$u(x,y,z) = \mathrm{Re}^{5/3}x^{-5/3}U(\eta,\xi),$$

$$v(x,y,z) = \mathrm{Re}^{1/3}x^{-4/3}V(\eta,\xi),$$

$$w(x,y,z) = \mathrm{Re}^{1/3}x^{-4/3}W(\eta,\xi),$$

$$p(x,y,z) = \mathrm{Re}^{2/3}x^{-8/3}P(\eta,\xi),$$

$$\eta = \frac{y\mathrm{Re}^{4/3}}{x^{4/3}}, \quad \xi = \frac{z\mathrm{Re}^{4/3}}{x^{4/3}}.$$

Thus, the thickness and width of the three-dimensional non-swirling laminar wall jet increases in proportion to $x^{4/3}$.

For a given shape and height above the surface of the outlet pipe cross-section, the characteristics of the laminar swirling wall jet will depend on several initial parameters specified in the jet outflow cross-section namely, the flow rate, the swirl, and the Reynolds number. We will determine the missing parameters. We will assume that the pipe from which the jet is blown is long enough so that the Poiseuille profile for the longitudinal velocity component and solid-body rotation for the azimuthal velocity v_φ are established in the cross-sections not close to the exit cross-section:

$$u = 2\left(1 - r^2\right), \quad v_\varphi = \Omega r. \tag{1.6}$$

Here, the dimensionless radius r is reckoned from the axis of the pipe, $\Omega_1 = \left(u_{1*}/a\right)\Omega$ is the angular velocity of rotation of fluid in the pipe, and it is taken into account that the average-flow-rate velocity is equal to $u_{1*} = 1$, and the maximum velocity is equal to $u_{\max} = 2$. By swirl number we mean the quantity $S = \Omega_1 a/u_{1\max} = \Omega/2$.

At exit of the pipe, the jet has the momentum J_x in the x-direction and the momentum J_z close to zero in the z-direction

$$J_x = \int_{-\infty}^{\infty}\int_{0}^{\infty} u^2 dydz, \quad J_z = \int_{-\infty}^{\infty}\int_{0}^{\infty} uwdydz.$$

Under the action of the friction forces of fluid against the rigid surface, the longitudinal momentum of the jet will decrease with increase in x, and the transverse momentum will first be acquired and then lost. From Eqs. (1.3) and (1.5) it follows that

$$\frac{\partial J_x}{\partial x} = -\frac{1}{\mathrm{Re}}\int_{-\infty}^{\infty}\left.\frac{\partial u}{\partial y}\right|_{y=0} dz, \quad \frac{\partial J_z}{\partial x} = -\frac{1}{\mathrm{Re}}\int_{-\infty}^{\infty}\left.\frac{\partial w}{\partial y}\right|_{y=0} dz.$$

We can formulate the following hypothesis: at large distances from the jet source, asymmetry in the jet caused by the rotation of fluid in the outlet cross-section will disappear, the evolution of the jet will not differ in any way from the evolution of a non-swirling jet, but due to the acquired lateral momentum, the jet will propagate not along the x axis, but along a straight line inclined to the x axis at a certain angle θ, and for the swirling jet the self-similarity parameter will coincide with the self-similarity parameter for the non-swirling jet, i.e., it will be equal to 4/3.

2. NUMERICAL SOLUTION

The Navier–Stokes equations (1.1) were solved numerically using the finite volume method. The convective terms were approximated using a second-order accuracy scheme with differences upstream of the flow, and the diffusion terms and the pressure were approximated using central differences of second-order accuracy. The momentum and pressure equations were solved jointly. The problem was solved as the pseudo-nonstationary one with a fixed pseudo-time step.

The simulation was carried out on a structured computational grid with a total number of cells 6×10^6. In Fig. 1 we have given the parameters of the computational domain and the geometric parameters of the pipe (the surface of the pipe is highlighted in gray); proportions between different sizes in Fig. 1 are not respected. The expanding computational domain makes it possible to concentrate most of the cells inside the jet core.

The following boundary conditions were set on the boundaries of the computational domain:

• in the initial cross-section (*5*), the profiles of the velocity components are specified in accordance with (1.6);

• on the horizontal rigid surface (*9*) and on the surfaces (internal and external) of the pipe (*6*), the no-slip condition is specified;

• on the side (*1*), (*2*), top (*3*), front (*7*, *8*) and exit (*4*) free boundaries the following condition is imposed

$$\frac{\partial u}{\partial \mathrm{n}} = \frac{\partial v}{\partial \mathrm{n}} = \frac{\partial w}{\partial \mathrm{n}} = 0.$$

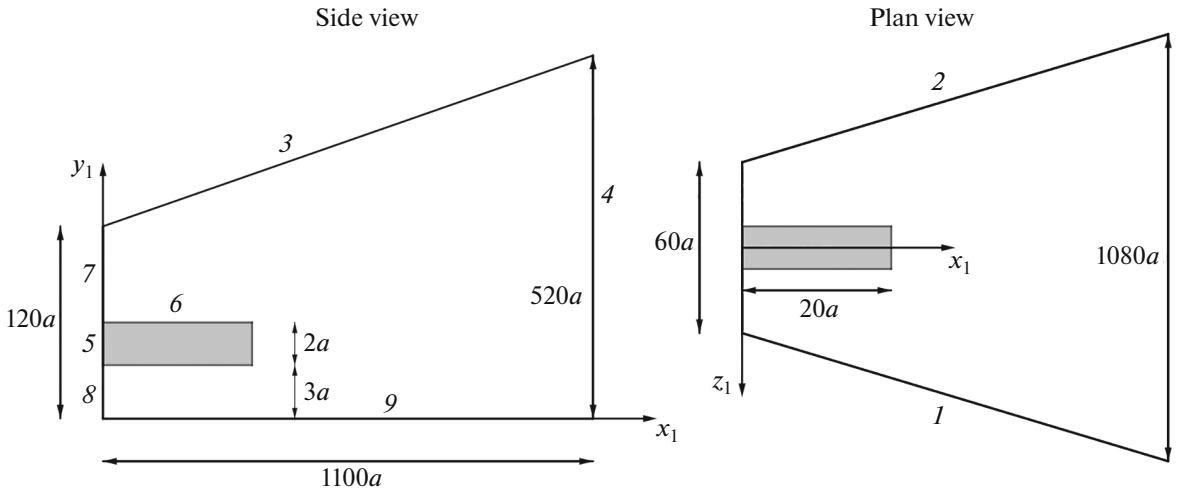

Fig. 1. Coordinate system of the problem and geometry of the computational domain.

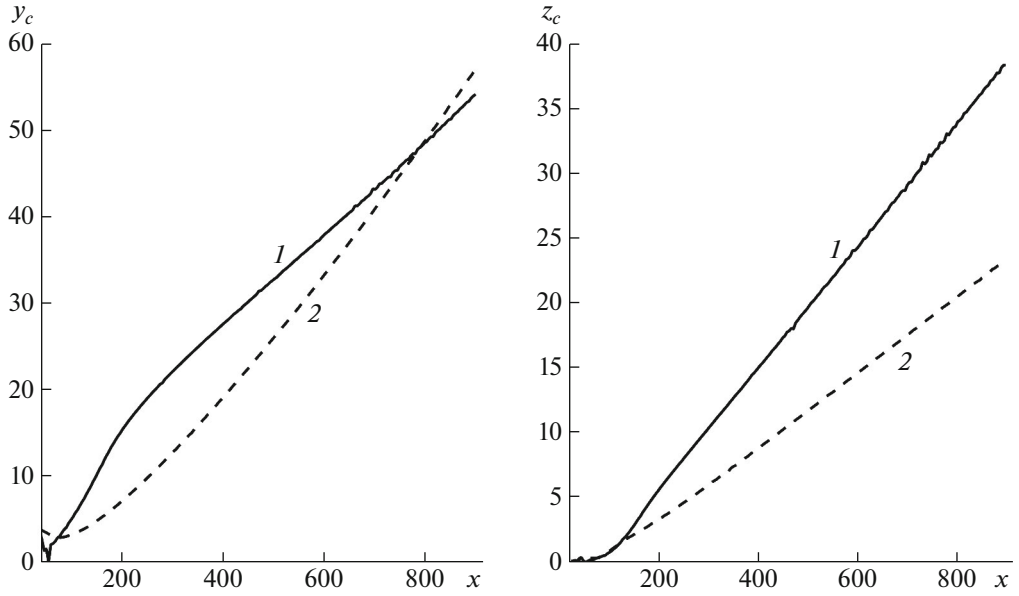

Fig. 2. Graphs of $y_c(x)$ and $z_c(x)$: curves *1* and *2* correspond to $S = 0.56$ and 0.33, respectively.

The establishment of a solution is monitored by the magnitude of the mass flow across the boundary (*4*) of the computational domain. In this case, the magnitude of the residuals in the momentum equation is not greater than 10^{-6}.

3. CALCULATION RESULTS

To be specific, we will assume that the center of the outlet pipe cross-section is located at the height $h_1 = 4a$ (Fig. 1). Two calculations were carried out at Re = 77, $S = 0.56$, and $S = 0.33$.

There is some arbitrariness in the choice of defining the center of the jet. In this work, the center of the jet in the cross-section $x = \text{const}$ is the point with coordinates $y_c(x)$, $z_c(x)$, at which the velocity component parallel to the rigid plane has a maximum, i.e., the function $\sqrt{u^2(x,y,z) + w^2(x,y,z)}$ has a maximum at a given x. In Fig. 2 we have reproduced the graphs of the functions $y_c(x)$ and $z_c(x)$, from which

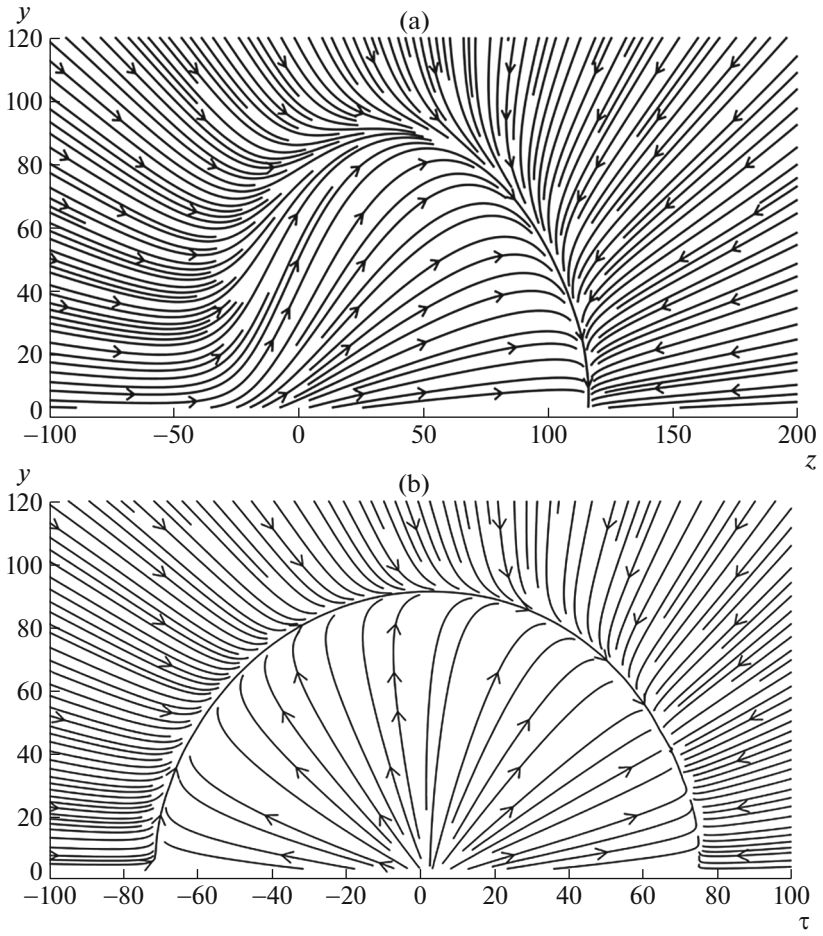

Fig. 3. (a) Cross-flow streamlines at Re = 77 and $S = 0.56$ in the cross-section $x = 600$ in the original coordinate system. (b) Cross-flow streamlines at Re = 77 and $S = 0.56$ in the cross-section $x = 600$ in the new coordinate system.

it follows that the jet actually propagates at a certain angle to the x axis. Obviously, this angle depends on the initial jet swirl. At $S = 0.33$ and 0.56 these angles are equal to 1.7° and 2.7°, respectively.

We introduce the concept of a cross-flow streamline in the cross-section $x = x_0 = \text{const}$. The streamline equation is as follows:

$$\frac{dy}{v(x_0, y, z)} = \frac{dz}{w(x_0, y, z)}.$$

In Fig. 3a have plotted the cross-flow streamlines at $x = 600$. If instead of coordinates x, y, z we introduce a coordinate system ζ, y, τ turned by an angle θ (Fig. 4), then in this coordinate system the cross-flow streamlines correspond to those shown in Fig. 3b. In Fig. 3b the streamlines correspond to similar calculations for the non-swirling jet [23]. For jet propagation along the ζ axis, a determined self-similarity parameter is equal to 4/3. This confirms the hypothesis on the correspondence of the evolution of the swirling jet turned by an angle θ in the far field to the evolution of the non-swirling jet.

4. ABSENCE OF THE STATIONARY SOLUTION AT LARGE S

Just as in the free jet, an increase in the jet swirl leads to appearance of recirculation flow regions in the flow [26]. When the reverse flow appears, the residuals when solving the time-independent Navier–Stokes equations can no longer be made less than a certain specified value. This fact indicates the need to solve the problem using the time-dependent Navier–Stokes equations.

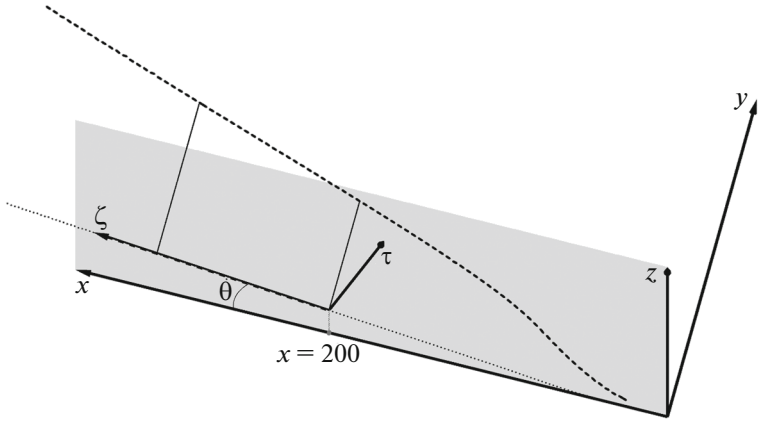

Fig. 4. Rectangular Cartesian coordinate systems x, y, z and ζ, y, τ. Dashed line corresponds to the line $y = y_c(x)$, $z = z_c(x)$, the points are the projection of the dashed line onto the plane $y = 0$. The ζ axis is directed along the tangent to the projection of the dashed line onto the plane $y = 0$ at point $x = 200$.

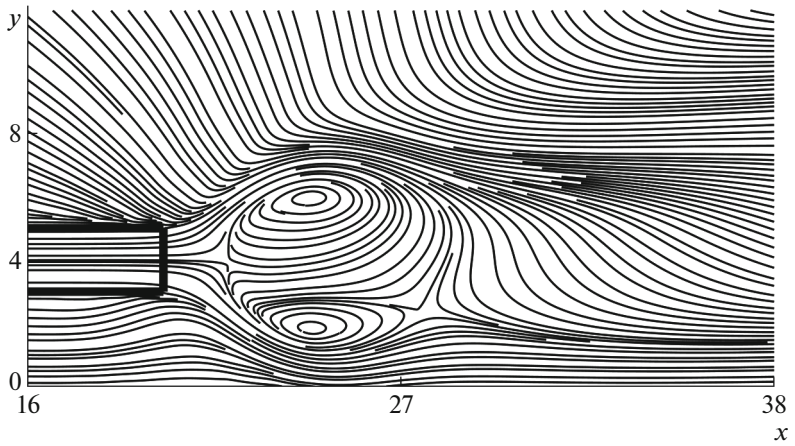

Fig. 5. Streamlines corresponding to the calculation at $S \approx 1.1$.

The calculation results are presented in Figs. 5 and 6 in the form of streamlines in the cross-section $z = 0$

$$\frac{dx}{u(x,y,0)} = \frac{dy}{v(x,y,0)}.$$

At $S \approx 1.1$, although a nonstationarity is present, but the streamline pattern depends on time only slightly (see Fig. 5). It is a different matter when the jet swirl becomes even greater, $S \approx 2.2$ (see Fig. 6). In this case, in the vicinity of the recirculation region, whose geometry strongly depends on time, additional vortices of different directions of rotation are formed. The flow becomes periodic. In Fig. 6 we have shown the characteristic change in the streamlines at regular intervals during the period. The flow periodicity can also be observed by changes in the longitudinal velocity component at a given point in space. As such, a point on the extension of the pipe axis spaced 4 radii from the outlet section was taken (see Fig. 7).

SUMMARY

For the first time, important distinctive features of the evolution of a three-dimensional swirling laminar jet have been determined. The jet swirl causes the jet to deviate from the original direction. In the far region, the jet propagates at a certain angle to this initial direction. The three-dimensional swirling wall jet quickly loses its swirl, and in a turned coordinate system its behavior in the far region differs only slightly from that of the non-swirling jet. Accordingly, the self-similarity parameter turns out to be the same as in the non-swirling jet, namely, it is equal to 4/3. The transverse dimensions of the jet increase

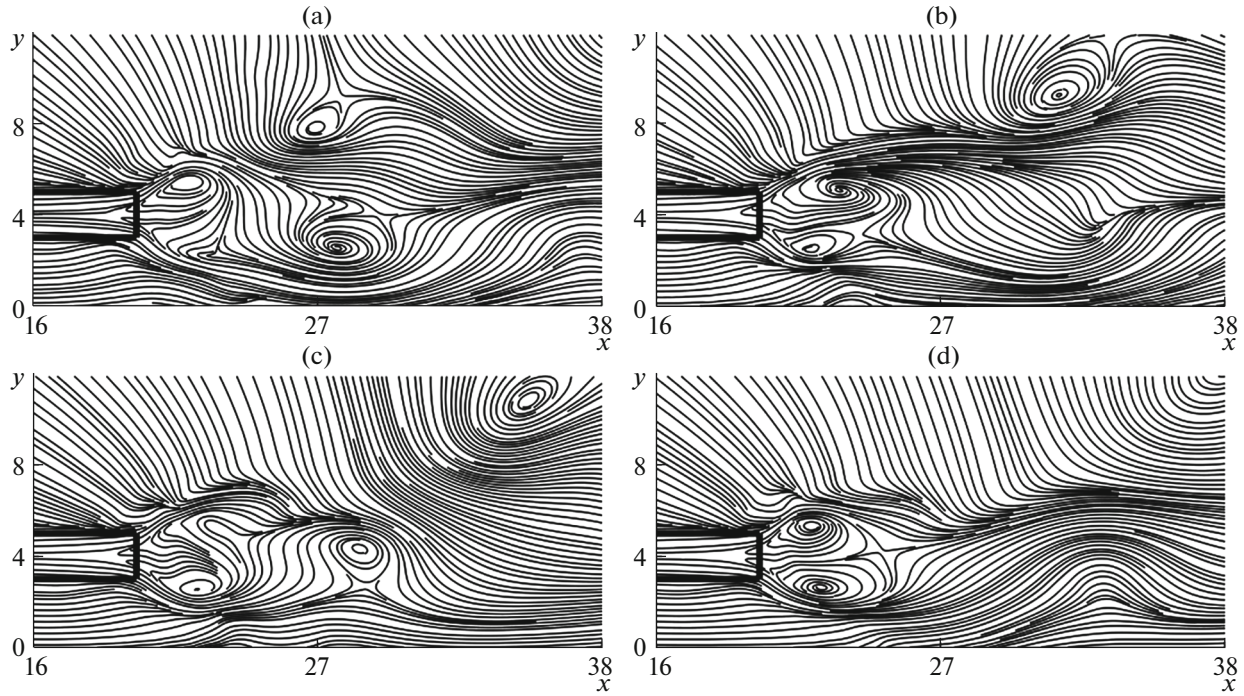

Fig. 6. Streamlines for the calculation at $S \approx 2.2$ that correspond to four different points in time during a single period in the chronological order.

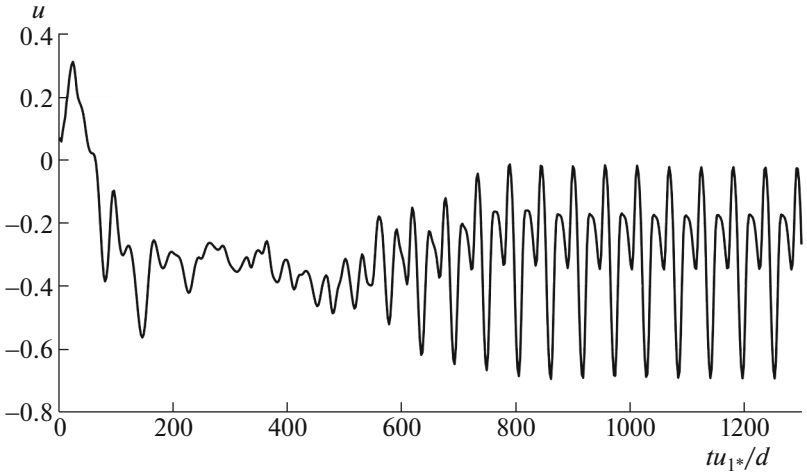

Fig. 7. Variation in the longitudinal velocity component at a fixed point in space in the neighborhood of the outlet pipe cross-section.

proportionally to $\zeta^{4/3}$, the longitudinal velocity component decays according to the law $\zeta^{-5/3}$, and the transverse components proportionally to $\zeta^{-4/3}$.

At high swirl, areas of recirculation flow appear in the jet. The flow becomes unsteady and periodic.

FUNDING

The scientific study was supported by the Russian Science Foundation Grant no. 23-11-00210, https://rscf.ru/project/23-11-00210/.

CONFLICT OF INTEREST

The authors of this work declare that they have no conflicts of interest.

OPEN ACCESS

REFERENCES

1. Wygnanski, I., Katz, Y., and Horev, E., On the applicability of various scaling laws to the turbulent wall jet, *J. Fluid Mech*., 1992.
2. Schneider, M.E. and Goldstein, R.J., Laser Doppler measurement of turbulence parameters in a two-dimensional plane wall jet, *Phys. Fluids,* 1994, vol. 6, pp. 3116–3129.
3. Eriksson, J., Karlsson, R., and Persson, J., An experimental study of a two-dimensional plane turbulent wall jet, *Exp. Fluids,* 1998.
4. Eriksson, J., *Experimental Studies of the Plane Turbulent Wall Jet: PhD Thesis*, Stockholm: Sweden: Royal Institute of Technology, Department of Mechanics, 2003.
5. Sun, H. and Ewing, D., Effect of initial and boundary conditions on development of three-dimensional wall jets, *40th AIAA ASME,* 2002, p. 733.
6. Agelin-Chaab, M. and Tachie, M.F., Characteristics of turbulent three-dimensional wall jets, *ASME, J. Fluids Eng.*, 2011, vol. 133, no. 2.
7. Namgyal, L. and Hall, J., Reynolds stress distribution and turbulence generated secondary flow in the turbulent three-dimensional wall jet, *J. Fluid Mech.*, 2016, vol. 800, pp. 613–644.
8. Inoue, Y., Yano, H., and Yamashita, S., Experimental study on a three-dimensional wall jet, *JFST*, 2007, vol. 2, no. 3, pp. 655–664.
9. Hall, J.W. and Ewing, D., Three-dimensional turbulent wall jets issuing from moderate-aspect-ratio rectangular channels, *AIAA J.*, 2007, vol. 45, pp. 1177–1186.
10. Newman, B., Patel, R., Savage, S., and Tjio, H., Three-dimensional wall jet originating from a circular orifice, *AEQ*, 1972, vol. 23, no. 3, pp. 188–200.
11. Matsuda, H., Iida, S., and Hayakawa, M., Coherent structures in a three-dimensional wall jet, *ASME. J. Fluids Eng.*, 1990, vol. 112, no. 4, pp. 462–467.
12. Padmanabham, G. and Lakshmana Gowda, B.H., Mean and turbulence characteristics of a class of three-dimensional wall jets. Part 1: Mean flow characteristics, *ASME. J. Fluids Eng.,* 1991, vol. 113, no. 4, pp. 620–628.
13. Pani, B.S. and Rajaratnam, N., Swirling circular turbulent wall jets, *JHR*, 1976, vol. 14, no. 2, pp. 145–154.
14. Dejoan, A. and Leschziner, M., Large eddy simulation of a plane turbulent wall jet, *Phys. Fluids*, 2005, vol. 17.
15. Naqavi, I.Z., Tyacke, J.C., and Tucker, P.G., Direct numerical simulation of a wall jet: flow physics, *J. Fluid Mech.*, 2018, vol. 852, pp. 507–542.
16. Gaifullin, A.M. and Shcheglov, A.S., Flow structure in a three-dimensional turbulent wall jet, *Prikl. Mat. Mekh.*, 2023, no. 2, pp. 226–239.
17. Craft, T. and Launder, B., On the spreading mechanism of the three-dimensional turbulent wall jet, *J. Fluid Mech.*, 2001, vol. 435, pp. 305–326.
18. Kakka, P. and Anupindi, K., Flow and thermal characteristics of three-dimensional turbulent wall jet, *Phys. Fluids,* 2021, vol. 33, no. 2.
19. Khosronejad, A. and Rennie, C.D., Three-dimensional numerical modeling of unconfined and confined wall-jet flow with two different turbulence models, *Can. J. Civ. Eng.*, 2010, vol. 37, no. 4, pp. 576–587.
20. Akatnov, N.I., Propagation of a plane laminar jet of viscous fluid along a solid wall, *Trudy Leningr. Politekhn. Inst.*, 1953, no. 5, pp. 24–31.
21. Glauert, M.B., The wall jet, *J. Fluid Mech.*, 1956, vol. 1, pp. 625–643.
22. Krechetnikov, R. and Lipatov, I., Hidden invariances in problems of two-dimensional and three-dimensional wall jets for Newtonian and non-Newtonian fluids, *SIAM J. Appl. Math.*, 2002, vol. 62, no. 6, pp. 1837–1855.

23. But, I.I., Gailfullin, A.M., and Zhvick, V.V., Far field of a three-dimensional laminar wall jet, *Fluid Dyn.,* 2021, vol. 56, no. 6, pp. 812–823. https://doi.org/10.1134/S0015462821060021
24. Barenblatt, G.I., *Avtomodel'nye yavleniya – analiz pazmernostei i skeiling* (Self-Similar Phenomena—Dimensional Analysis and Scaling), Dolgoprudnyi: Intellekt, 2009.
25. Gaifullin, A.M. and Zhvick, V.V., Interaction between two oppositely swirled submerged jets, *Fluid Dyn.,* 2019, vol. 54, no. 3, pp. 339–348. https://doi.org/10.1134/S001546281902006X
26. Zhvick, V.V., Invariants and asymptotics of axisymmetric swirling submerged jets, *Zh. Prikl. Mekh. Tekh. Fiz.*, 2020, vol. 61, no. 2, pp. 92–108.

Translated by E.A. Pushkar